ACS APPLIED ELECTRONIC MATERIALS

pubs.acs.org/acsaelm Article

Electrospun P(VDF-TrFE):$LiClO_4$ Hybrid Nanofiber-Based Highly Sensitive Piezocapacitive Pressure Sensors for Self-Powered Flexible Electronics

Pankaj Kumar, Ranbir Singh, and Satinder K. Sharma*

Cite This: https://doi.org/10.1021/acsaelm.5c00199 Read Online

ACCESS | Metrics & More | Article Recommendations

ABSTRACT: Piezoelectric materials are extensively utilized in energy harvesters, accelerometers, dynamic pressure sensing, and pulse sensing applications. Here, we developed a flexible piezocapacitive pressure sensor utilizing electrospun P(VDF-TrFE):$LiClO_4$ (polyvinylidene fluoride-*co*-tetrafluoroethylene: lithium perchlorate) hybrid nanofibers for innovative sensing applications. The developed sensor offers an alternative technique for overcoming the constraints of conventional pressure sensors by employing the distinctive piezoelectric properties of P(VDF-TrFE) nanofibers and enhanced electric conductivity due to doped lithium perchlorate ($LiClO_4$). The excellent sensing, enabled by the incorporation of $LiClO_4$ in P(VDF-TrFE), was extensively investigated through multiscale testing. Piezoresponse force microscopy (PFM) and a d_{33} piezometer were used to assess the piezoelectric characteristics of nanofibers. The P(VDF-TrFE):$LiClO_4$ hybrid nanofibers have shown ∼21% enhancement in the piezoelectric coefficient (d_{33}) and a substantial increase in output voltage (∼1.4 V) for an optimal concentration of $LiClO_4$ (5 w/v%). Functionality of the developed sensory system has been demonstrated by precisely monitoring the radial artery pulse pressure and measuring capacitance versus time waveform that was analogous to arterial pulse dynamics. This technique highlights the potential of P(VDF-TrFE):$LiClO_4$ nanofiber-based sensors for real-time noninvasive health monitoring. The prototype sensor exhibits a rapid response and relaxation time of ∼20−30 ms and a sensitivity of 6.639 kPa^{-1}. The developed pressure sensory system opens the way for next-generation wearable biomedical devices, establishing a benchmark for future advancement in E-skin, wearable electronics, medical surveillance, and automation systems.

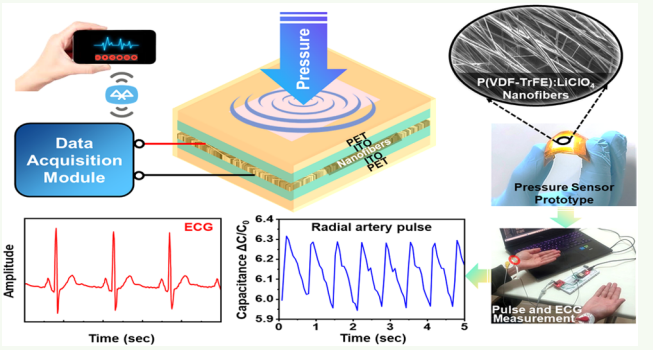

KEYWORDS: *P(VDF-TrFE), hybrid nanofibers, piezocapacitive pressure sensor, electrospinning, self-powered wearables, flexible, pulse sensor, wireless transmission*

INTRODUCTION

Wearable and flexible electronics are transforming numerous applications, including displays, futuristic automobiles, robotics, energy generation, e-skin, biomedical devices, and the Internet of Things (IoTs).[1−7] Pressure sensors play a vital role in a variety of commercial, healthcare, and scientific applications, facilitating precise measurement of mechanical stimuli forces and real-time monitoring and control of physiological functionality. Despite being efficient in many scenarios, conventional pressure sensors encounter challenges related to sensitivity, flexibility, and adaptability to diverse ambient conditions. As technology advances, the quest for intelligent, multifunctional pressure sensors capable of addressing these constraints and delivering improved performance and functionality has become increasingly crucial.

Capacitive and piezoelectric pressure sensors are often used, mainly due to their low power consumption, stability, and simple design. In spite of their utility, these sensors typically exhibit limited sensitivity and incompatibility with flexible electronics. To improve sensitivity, conductive fillers such as carbon nanotubes,[8−10] graphene,[11−13] and metal nanowires[14−17] were incorporated into the elastomer to augment the change in dielectric constant when applied external pressure. However, the sensitivity improvements were merely insignificant. Various tweaks to the structure, such as pyramid structures and[14,18−20] micropillar structures,[21−23] aimed to improve sensitivity but showed a rapid decrease in sensitivity as the function of pressure. Furthermore, the use of porous

Received: January 28, 2025
Revised: June 6, 2025
Accepted: June 9, 2025

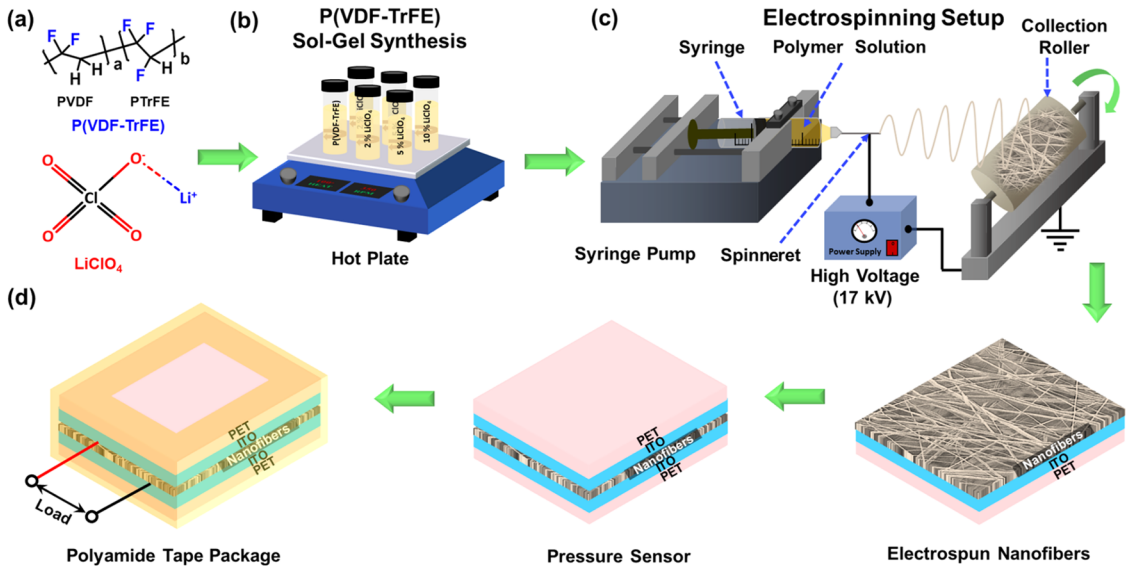

Figure 1. Schematic illustration of process flow for nanofiber-based pressure sensor fabrication. (a) Chemical structures of polyvinylidene fluoride-trifluoroethylene and lithium perchlorate, (b) synthesis of P(VDF-TrFE):$LiClO_4$ solution, (c) electrospinning methodology for nanofibers synthesis, and (d) packaging of pressure sensor device in polyamide tape.

elastomers[15,24−26] was intended to improve sensor sensitivity by facilitating easier compression in contrast to nonporous counterparts. Recently, ionic hydrogels with high ionic conductivity have been introduced onto the dielectric layer within the sensor to form electrical double-layer capacitors on the electrode surface.[25,27−29] However, the hydrogel's vulnerability to dehydration, especially in the absence of an elastomeric coating, directly jeopardizes sensor durability.

Recently, the incorporation of unconventional materials and distinctive fabrication methods has opened promising prospects for the development of highly sensitive and receptive pressure sensory systems.[30−34] In this context, the incorporation of lithium perchlorate ($LiClO_4$) as an electrolyte into P(VDF-TrFE) nanofiber-based sensors can enhance the sensor's performance and functionality by improving electrical conductivity. These advancements are poised to address and overcome the drawbacks of existing analogous sensing systems.[35,36] The unique strategy of this combination of P(VDF-TrFE) and lithium perchlorate hybrid nanofibers offers a promising framework for the development of piezocapacitive flexible pressure sensors that can detect mechanical fluctuations in applied pressure.

This work examines the potential applications of P(VDF-TrFE):$LiClO_4$ hybrid electrospun nanofiber-based pressure sensor systems. The unique attributes of P(VDF-TrFE) nanofibers, such as piezoelectricity and flexibility, contribute to the excellent sensing ability and adaptability of the developed sensory systems. The inclusion of lithium perchlorate further significantly improves the efficacy by increasing the electrical conductivity and receptivity.

Owing to the simple structure, low-cost processing, and superior performance of the developed sensors, they are viable candidates for applications, including flexible electronics, biosensing, energy storage, healthcare monitoring, and automation systems.

RESULTS AND DISCUSSION

The chemical structures of poly(vinylidene fluoride)-trifluoroethylene (P(VDF-TrFE)) and lithium perchlorate ($LiClO_4$) are illustrated in Figure 1a. The emergence of electrospun hybrid P(VDF-TrFE) nanofibers has introduced exciting possibilities for enhancing sensing capabilities in the field of pressure sensor technology. Traditional materials such as PVDF and P(VDF-TrFE) have demonstrated potential, but their performance frequently fails to meet expectations. P(VDF-TrFE) is known for its exceptional properties, including elevated remnant polarization, resulting in an improved electromechanical coupling factor. Consequently, there is a higher efficiency in detecting the mechanical pressures.[37] One notable characteristic of P(VDF-TrFE) in pressure sensors is its piezoelectric feature. This property is mainly attributed to its β-phase content, rendering it suitable for developing pressure sensors and piezoelectric nanogenerators (PENGs).[38] In this context, the incorporation of $LiClO_4$ as a dopant in the electrospun P(VDF-TrFE) nanofibers due to its strong dissociation tendency and ability to intercalate within the nanofibers leads to an increase in electrical conductivity and piezoelectric response. Ionic interactions promote dipolar orientation and polarization under mechanical stress, which are crucial for pressure sensing applications. $LiClO_4$ also causes nanofiber microphase separation, improving piezoelectric performance. Recent studies have been dedicated to enhancing the distribution of lithium ions within the polymer matrix to maximize the internal electric field and improve the performance of nanofiber-based pressure sensors.[39,40]

The electrospinning approach synthesized the hybrid nanofibers of P(VDF-TrFE):$LiClO_4$, as shown in Figure 1, with the formulation process flow detailed in the experimental segment. The nanofibers were annealed at 125 °C to enhance their crystallinity, as reported elsewhere. This annealing process between the melting and Curie temperatures occurs within the paraelectric phase and enhances the crystallinity by ~70%.[37] Subsequently, during the fabrication process, the electrospun nanofibers of P(VDF-TrFE):$LiClO_4$ were subjected to morphological, electrical, and piezoelectric characterizations.

https://doi.org/10.1021/acsaelm.5c00199
ACS Appl. Electron. Mater. XXXX, XXX, XXX−XXX

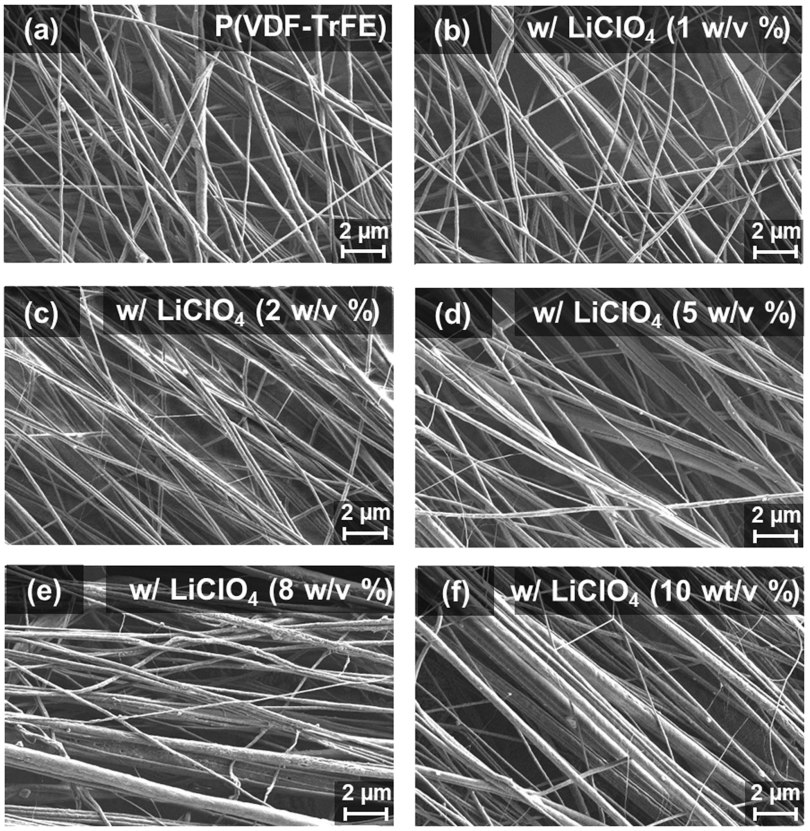

Figure 2. (a–f) FESEM micrographs of P(VDF-TrFE):$LiClO_4$ hybrid nanofibers at various $LiClO_4$ concentrations.

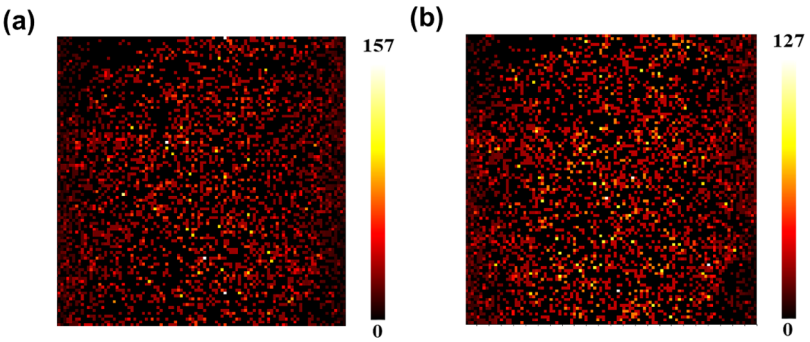

Figure 3. X-ray photoelectron spectroscopy (XPS) elemental mapping images of (a) Li and (b) Cl.

Morphological Analysis. A field emission scanning electron microscope (FESEM) was used to examine the P(VDF-TrFE) and P(VDF-TrFE):$LiClO_4$ hybrid nanofibers for morphological characterization. FESEM micrographs of pure P(VDF-TrFE) and P(VDF-TrFE):$LiClO_4$ hybrid nanofibers synthesized with different $LiClO_4$ concentrations (1, 2, 5, 8, and 10 w/v%) are shown in Figure 2. As per the statistical analysis of numerous nanofibers obtained from multiple FESEM images for each sample, the average diameters of pure P(VDF-TrFE) and P(VDF-TrFE):$LiClO_4$ (5 w/v%) nanofibers were approximately 133.50 and 146.97 nm, respectively. Further, the results indicated that as the $LiClO_4$ proportion rose to 5 w/v%, the fiber surfaces were uniform and devoid of beads. Meanwhile, higher $LiClO_4$ concentrations over 5% (w/v) led to elevated surface roughness and bead-like accumulations. Moreover, in order to confirm the homogeneous incorporation of $LiClO_4$ into PVDF-TrFE nanofibers, X-ray photoelectron spectroscopy (XPS) elemental mapping was performed. Figure 3a,b depicts the spatial distributions of Li and Cl within the nanofibers. The elemental maps show a uniform distribution of Li and Cl in the nanofiber matrix, signifying the effective incorporation of $LiClO_4$ on the molecular scale.

Structural and Spectroscopic Analysis. X-ray diffraction (XRD) spectra were analyzed to further investigate the polymorphism of the P(VDF-TrFE):$LiClO_4$ hybrid nanofibers. The XRD pattern of pure $LiClO_4$ salt shows distinct crystalline peaks, with the most prominent peak observed around 35° in the 2θ range (Figure 4a). Figure 4a illustrates the XRD spectra for pure P(VDF-TrFE) and hybrid nanofibers doped with $LiClO_4$ (1–10 w/v%). The β-phase of P(VDF-TrFE) exhibited prominent diffraction peaks around 20°, corresponding to Bragg diffraction from the 110/200 planes of the crystalline β-phase. The nonpolar α-phase (020) observed around 18.2° in the 2θ range appears relatively weak and lacks

https://doi.org/10.1021/acsaelm.5c00199
ACS Appl. Electron. Mater. XXXX, XXX, XXX–XXX

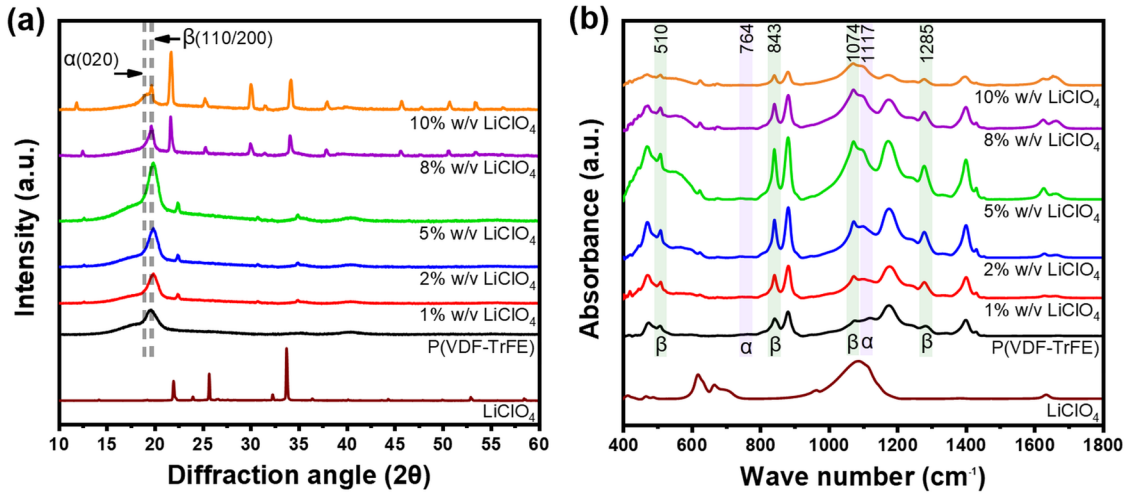

Figure 4. (a) XRD patterns and (b) FTIR spectra of pure $LiClO_4$ and P(VDF-TrFE) nanofibers with different concentrations of $LiClO_4$ (0−10 w/v%).

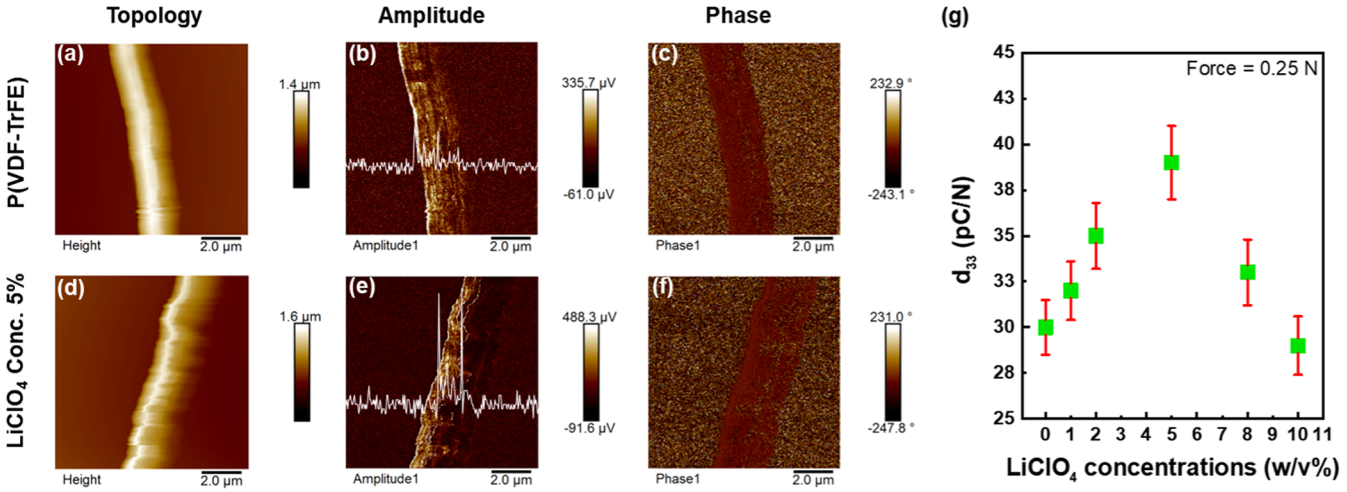

Figure 5. PFM scanned pictures of single P(VDF-TrFE) and P(VDF-TrFE):$LiClO_4$ hybrid nanofibers with topology, amplitude, and phase (a−c) P(VDF-TrFE), (d−f) $LiClO_4$ concentration 5 w/v%, and (g) d_{33} behavior of nanofibers for varying concentrations of $LiClO_4$.

significant prominence. The β-phase content (F_β) was ascertained by applying the following equation.[41]

$$F_\beta = \frac{I_\beta}{I_\alpha + I_\beta} \times 100\% \quad (1)$$

The diffraction peak intensities for the α- and β-phases are represented by I_α and I_β, respectively. Pure P(VDF-TrFE) nanofibers exhibited a β-phase of 69.44% (I_α = 1863.77, I_β = 4234.67), while $LiClO_4$ doping (5 w/v%) increased the β-phase content to 76.50% (I_α = 3153.63, I_β = 10265.81), signifying an improved formation of the polar crystalline β-phase. The XRD spectrum of hybrid nanofibers with an optimal $LiClO_4$ concentration (5 w/v%) showed a significant increase in peak intensity corresponding with the β-phase relative to pure P(VDF-TrFE) nanofibers. This enhancement indicates the polymer chain alignment into the all-trans conformation of the β-phase. These findings demonstrate that $LiClO_4$ doping significantly boosts the β-phase content in P(VDF-TrFE):$LiClO_4$ hybrid nanofibers essential for enhancing the piezocapacitive performance in pressure sensors.

FTIR spectroscopy was used to analyze the phase composition and molecular interactions in the P(VDF-TrFE) nanofibers doped with $LiClO_4$. The spectra (Figure 4b) indicate prominent peaks of the β-phase, notably a significant absorption band at 843 cm^{-1}, which corresponds to the C−F stretching vibration of the polar crystalline structure; a peak at 1285 cm^{-1} demonstrates the significant β-phase, while the α-phase band around 764 and 1117 cm^{-1} is considerably less pronounced.

The elevated β-phase intensity in $LiClO_4$-doped (5 w/v%) nanofibers indicates a significant interaction between lithium ions (Li^+) and the polymer matrix. Lithium ions interact with the fluorine atoms of P(VDF-TrFE), forming localized electric fields that aid in the alignment of the dipoles in polymer chains. This interaction stabilizes the β-phase, which is crucial for improved piezocapacitive characteristics. The prevalence of the β-phase in the FTIR spectra emphasizes the efficiency of $LiClO_4$ doping in altering the structural attributes of P(VDF-TrFE) nanofibers for improved piezocapacitive response.

PFM Analysis. The piezoresponse force microscopy (PFM) technique was used to assess the piezoelectric properties in pure P(VDF-TrFE) and P(VDF-TrFE):$LiClO_4$ nanofibers with different concentrations of $LiClO_4$ (1−10 w/v%). Topology, amplitude, and phase-contrast images of the

https://doi.org/10.1021/acsaelm.5c00199
ACS Appl. Electron. Mater. XXXX, XXX, XXX−XXX

P(VDF-TrFE) and hybrid nanofibers infused with optimum concentration of $LiClO_4$ (5 w/v%) are shown in Figure 5a–f, respectively. An AFM probe tip with 1.6 V harmonic V_{ac} scanned individual P(VDF-TrFE) and P(VDF-TrFE):$LiClO_4$ hybrid nanofibers with a 5 × 5 μm^2 area. The amplitude image has a high piezoelectric contrast due to AC field deflection, where brighter regions indicate a higher piezoresponse than dark regions.[42] The P(VDF-TrFE):$LiClO_4$ hybrid nanofiber phase image reveals both negative and positive contrasts, demonstrating antiparallel ferroelectric nanodomains' presence and associated domain walls. The dark regions correspond to the negative domains having downward alignment and perpendicular polarization to the surface of the nanofiber, while bright spots correspond to the positive domains having upward alignment and perpendicular polarization relative to the surface of the nanofiber. The clearly discernible piezoelectric domains and extended crystallites indicate a uniform β-phase.[43] Thus, the nanodomains in the P(VDF-TrFE):$LiClO_4$ hybrid nanofiber are oriented perpendicularly to the nanofiber along the z-axis direction. The PFM signal is essentially nonpolar, suggesting that polar-phase nanocrystals have a higher piezoelectric response perpendicular to the axis of nanofiber. The hybrid P(VDF-TrFE):$LiClO_4$ nanofibers exhibit a greater piezoelectricity than the pure P(VDF-TrFE) nanofibers.

Furthermore, the d_{33} (piezoelectric coefficient) measurement was performed to determine the volumetric change in the piezoelectric material and the consequent polarization owing to pressure. The d_{33} piezometer was used to evaluate the d_{33} coefficient of both pure P(VDF-TrFE) and P(VDF-TrFE):$LiClO_4$ hybrid nanofibers at varying $LiClO_4$ concentrations (1–10 w/v%). Figure 5g indicates notable variations in the d_{33} coefficient for both pure P(VDF-TrFE) and P(VDF-TrFE):$LiClO_4$ hybrid nanofibers doped with various $LiClO_4$ concentrations. $LiClO_4$ concentration of up to 5 w/v% caused a significant rise in the d_{33} value. However, increasing the $LiClO_4$ concentration to over 5% led to a reduction in the d_{33} value of the P(VDF-TrFE):$LiClO_4$ hybrid nanofibers. This decreasing trend means that the piezoelectric characteristics of the hybrid nanofibers will be saturated and impaired at greater $LiClO_4$ concentrations; the excess $LiClO_4$ leads to particle aggregation, hindering polarization and reducing piezoelectric performance.

Sensing Mechanism. P(VDF-TrFE) is a copolymer that has excellent ferroelectric and piezoelectric properties, owing to the intrinsic dipole moments induced by the C–F and C–H bonds because of electronegativity differences. These dipoles can realign due to external forces, such as electric fields or mechanical stress, leading to polarization. Lithium perchlorate ($LiClO_4$) dissociates in the polymer matrix into Li^+ (cations) and ClO_4^- (anion). The small size and high charge density of Li^+ ions enable them to localize nearby electronegative fluorine atoms in P(VDF-TrFE) chains, resulting in an increased level of polarization. The larger and more spatially dispersed ClO_4^- ions generate diffuse electrostatic fields, altering the local polarization environment of the polymer matrix. These fields stabilize the dipoles of P(VDF-TrFE) in the β-phase and serve as a prepolarization force by aligning dipoles in the polymer matrix and thereby lowering the energy required to induce dipole reorientation. Under mechanical stress, Li^+ ions orient with negatively charged dipoles (fluorine atoms) on P(VDF-TrFE) chains. ClO_4^- ions dynamically alter the local electric environment under stress by generating transient electrostatic fields. Stress-induced reconfiguration/rearrangement of dipoles and ClO_4^- ions increase the piezocapacitive response of P(VDF-TrFE):$LiClO_4$ hybrid nanofibers, rendering them highly responsive to mechanical pressure. The schematic of the ionic interaction for P(VDF-TrFE):$LiClO_4$ and the fundamental sensing mechanism of piezocapacitive pressure sensors before applying pressure and under applied external pressure are shown in Figure 6a–c.

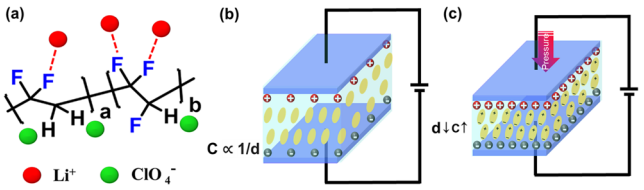

Figure 6. (a) Schematic of ionic interaction for P(VDF-TrFE) and $LiClO_4$, (b) sensing mechanism of piezocapacitive pressure sensors before applying pressure, and (c) under applied external pressure.

Electrical Properties Analysis. To evaluate the electrical characteristics of the fabricated pressure sensor, a Keithley 4200A-SCS parameter analyzer was employed. The externally applied pressure induces the charge separation within the electrospun P(VDF- TrFE):$LiClO_4$ hybrid nanofibers systems, generating a voltage output between the electrodes. This phenomenon occurs due to the piezoelectric behavior of the P(VDF-TrFE) material composite. The piezoelectric efficiency of the developed sensors was assessed by measuring its output voltage under preset conditions. The sensor was subjected to repeated compression and release pressure ranges of 124.05–243.78 Pa. This experiment yielded a steady and sequential output of alternately positive and negative voltage peaks, indicating that the sensor responds consistently. The output voltage response for pressure sensor devices incorporating pure P(VDF-TrFE) and P(VDF-TrFE):$LiClO_4$ hybrid nanofibers under the varying pressures and bending-releasing mode at 45° bending angle is shown in Figure 7a,b, respectively. $LiClO_4$, being an ionic compound, introduces lithium ions (Li^+) into the P(VDF-TrFE) nanofibers. The presence of these ions plays a significant role in enhancing the electrical conductivity of the nanofibers. When subjected to external pressure, the ions in the nanofibers experience changes in movement and alignment, resulting in a pressure sensor device doped with the optimal $LiClO_4$ concentration (5 w/v%) exhibiting a substantial increase (~1.4 V) in output voltage. Initially, the voltage rises as the concentration of $LiClO_4$ elevates to 5 w/v %. However, when the concentration of $LiClO_4$ exceeds 5 w/v %, the voltage of hybrid nanofibers decreases. A device setup configured with one stationary arm and the other adjustable arm was employed to study the electrical response of the fabricated pressure sensor devices under bending at a certain angle, as illustrated in Figure 12b. The experimental findings indicate that introducing $LiClO_4$ into P(VDF-TrFE) improves the piezoelectric characteristics of P(VDF-TrFE):$LiClO_4$ hybrid nanofibers.

Capacitance–time (C–T) study was conducted on P(VDF-TrFE) nanofiber-based sensors infused with varying concentrations (0, 1, 2, 5, 8, and 10 w/v%) of $LiClO_4$ to assess the relative change in capacitance under applied pressures and bending-releasing mode, providing crucial insights into the dynamic response of fabricated pressure sensors (Figure 8a,b). Experimental results revealed distinct variations in capacitance,

https://doi.org/10.1021/acsaelm.5c00199
ACS Appl. Electron. Mater. XXXX, XXX, XXX–XXX

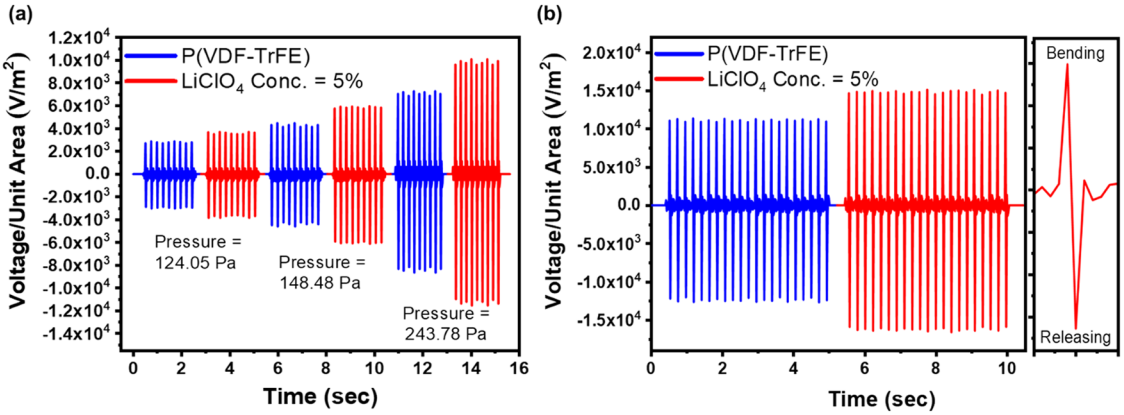

Figure 7. Piezoelectric output voltage waveforms for pure P(VDF-TrFE) nanofibers and P(VDF-TrFE):$LiClO_4$ hybrid nanofiber-based pressure sensor devices ($LiClO_4$ concentration = 5 w/v%). (a) Under the application of external pressures and (b) bending-releasing mode at 45° bending angle.

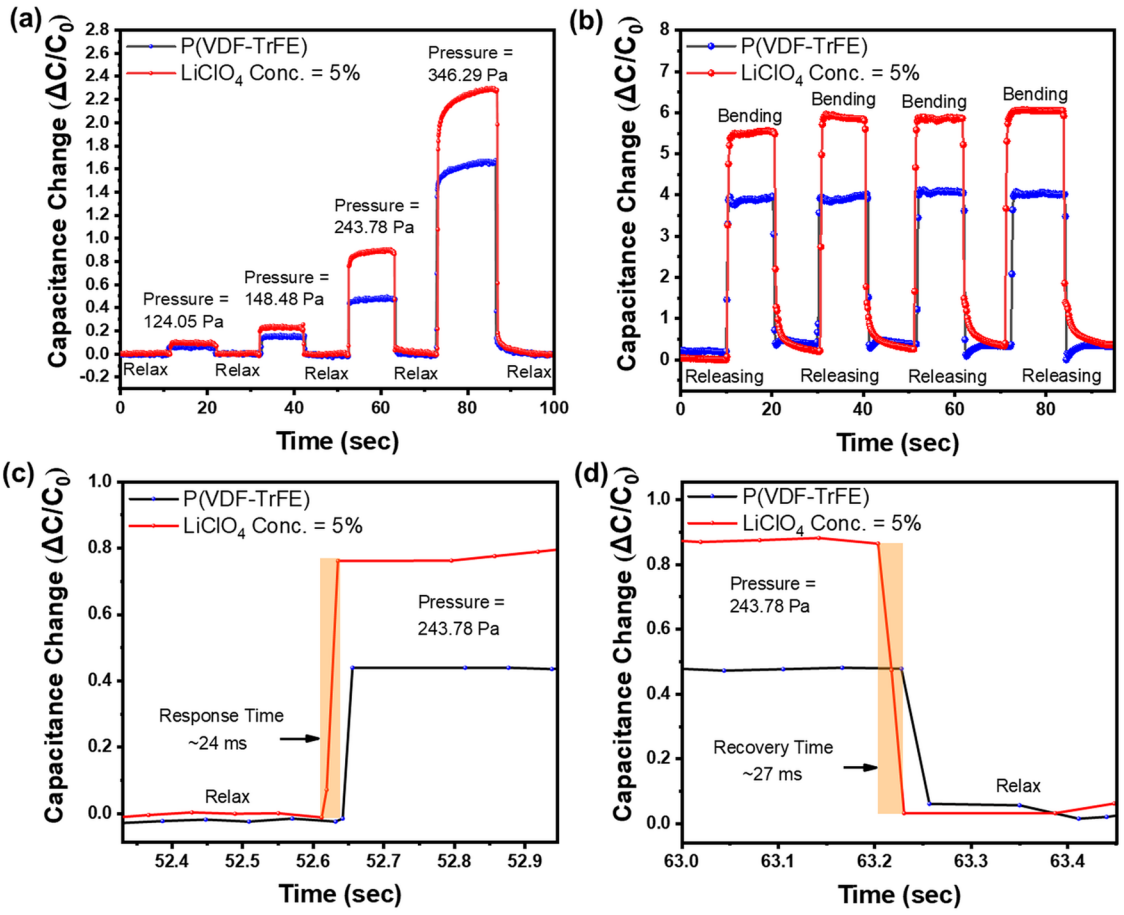

Figure 8. Relative change in capacitance ($\Delta C/C_0$) for pure P(VDF-TrFE) and P(VDF-TrFE):$LiClO_4$ sensors. (a) Under application of varying pressures, (b) bending-releasing mode at 45° bending angle, and (c, d) measured transient response of the pure P(VDF-TrFE) and P(VDF-TrFE):$LiClO_4$ sensors under an applied pressure of 243.78 Pa.

illustrating the profound influence of $LiClO_4$ on the electrical response dynamics of the sensors. Notably, sensors with a 5 w/v% concentration of $LiClO_4$ exhibited rapid response and recovery time (~20−30 ms) to pressure variations, as shown in Figure 8c,d. Conversely, sensors with pure P(VDF-TrFE) have shown slower and less pronounced responses. The P(VDF-TrFE) sensor showed a sensitivity of 5.835 kPa^{-1}, while the $LiClO_4$-doped (5 w/v%) sensor exhibited an increased sensitivity of 6.639 kPa^{-1}. The variations in sensitivity arise due to the intricate interplay between $LiClO_4$ concentrations and the nanofibers, where a 5% concentration likely facilitates improved ion migration and polarization, enhancing the response of the pressure sensor. However, at 10% concentration, excessive electrolyte content hinders ion mobility, leading to reduced receptivity. The P(VDF-TrFE):$LiClO_4$ hybrid nanofiber-based sensor ($LiClO_4$ conc. 5 w/v%) has been evaluated for reliability and durability under various vibration frequencies and cyclic pressure of 243.78 Pa, as

https://doi.org/10.1021/acsaelm.5c00199
ACS Appl. Electron. Mater. XXXX, XXX, XXX−XXX

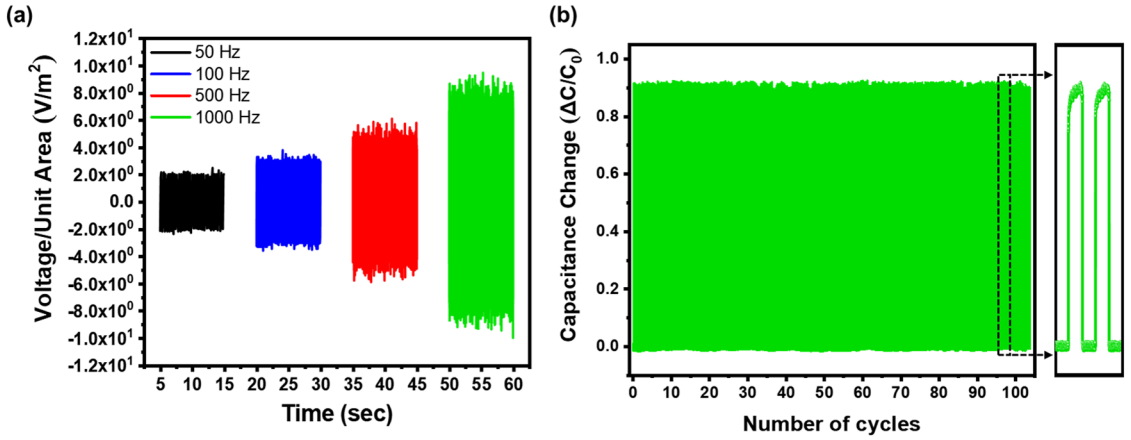

Figure 9. Output signal of P(VDF-TrFE):$LiClO_4$ hybrid nanofiber-based pressure sensor. (a) At different vibration frequencies and (b) under a cyclic pressure of 243.78 Pa.

shown in Figure 9a,b. The stable response observed in the resulting signals across varied vibration frequencies demonstrates the durability and ability of the sensor to operate reliably under dynamic loading scenarios. Similarly, the sensor exhibited excellent repeatability under cyclic pressure with no noticeable decline in signal amplitude or performance across numerous loading cycles. Figure 10 compares the dynamic

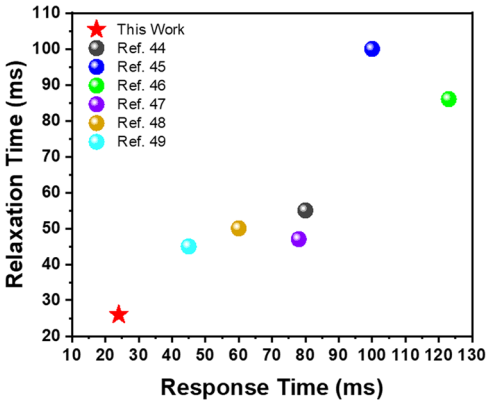

Figure 10. Comparison of response and relaxation times for the developed P(VDF-TrFE):$LiClO_4$ piezocapacitive pressure sensor (red star) and state-of-the-art sensors from the existing literature.

performance of developed P(VDF-TrFE):$LiClO_4$ piezocapacitive pressure sensor (red star) against existing sensors from the literature.[44−49] The developed sensor demonstrates superior performance with approximately 26 ms response and relaxation times, significantly outperforming existing referenced sensors that show response and relaxation times of 40−120 ms. This outstanding temporal responsiveness facilitates real-time detection of rapid pressure changes, which makes it optimal for wearable health monitoring and tactile sensing applications where speed is critical.

In addition, we showed the prototype pressure sensor designed to measure artery pulse pressure and compared it to ECG, the gold standard for heart rate (HR) and heart rate variability (HRV). Figure 11a−d represents a comprehensive evaluation of arterial pulse and ECG signal measurements, demonstrating the capability of the prototype pressure sensor to detect radial artery pulse signals. Figure 11a depicts the recorded waveform of the arterial pulse signal, reflecting mechanical fluctuations of blood traverses within the radial artery, whereas Figure 11b shows the typical waveform of the radial artery pulse, emphasizing distinct phases such as the systolic and diastolic peaks, along with the P-wave, T-wave, and D-wave, which signify the various stages of the pulse cycle. Figure 11c presents the wrist pulse measurement setup featuring the Keithley 4200A-SCS parameter analyzer and delineates the experimental configuration for precise signal acquisition. Ultimately, Figure 11d compares the recorded arterial pulse signal to the measured ECG waveform, where peak-to-peak interval (PPI), pulse transit time (PTT), and R-R Interval (RRI) can be identified on the corresponding waveforms in order to illustrate the temporal correlation between the pulse signal and the electrical activity of the heart. During experiments, the prototype sensor was affixed to the wrist, while three ECG electrodes were positioned on both the arms and the right leg (Figures 11c and 12c). This investigation reinforces the efficacy of the pressure sensor prototype in capturing and correlating the radial artery pulse wave to the electrical activity of the heart, demonstrating its reliability for pulse monitoring applications.

The images of the fabricated prototype pressure sensor device using P(VDF-TrFE):$LiClO_4$ hybrid nanofibers and the characterization setup are depicted in Figure 12. Figure 12a shows the assembled pressure sensor device being held in the hand, demonstrating its physical size (6.25 cm^2) and flexibility. The experimental arrangement for evaluating the electrical properties is depicted in Figure 12b. The AD8232 ECG sensor module was employed for measuring the ECG signal for comparison and correlation with the arterial pulse signal waveform, as illustrated in Figure 12c. Further, Figure 12d displays the ability of the sensor to communicate/transmit data wirelessly. This feature and functionality were enabled by employing an ESP-32 microcontroller integrated with Bluetooth and an Arduino IDE, which allows for remote data transfer from the pressure sensor prototype. This characteristic emphasizes the sensor utility in pressure sensing systems based on wireless surveillance systems.

CONCLUSIONS

In conclusion, a flexible and piezocapacitive pressure sensor was successfully developed by using electrospun P(VDF-TrFE):$LiClO_4$ hybrid nanofibers. Employing the synergistic properties of piezoelectric P(VDF-TrFE) nanofibers and

https://doi.org/10.1021/acsaelm.5c00199
ACS Appl. Electron. Mater. XXXX, XXX, XXX−XXX

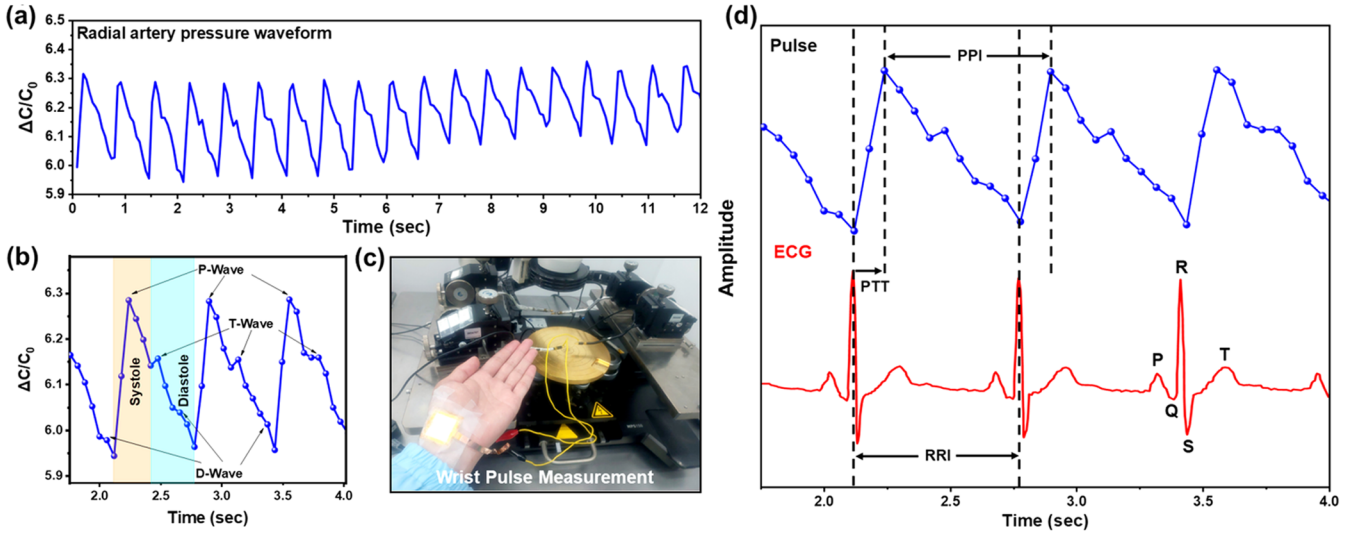

Figure 11. (a) Capacitance variation recorded in response to the radial artery pulse. (b) Magnified view of the pulse waveform, highlighting its distinct characteristic peaks. (c) Image showing the sensor positioned on the wrist. (d) Typical pulse signal acquired from the prototype device and measured ECG signal (bottom).

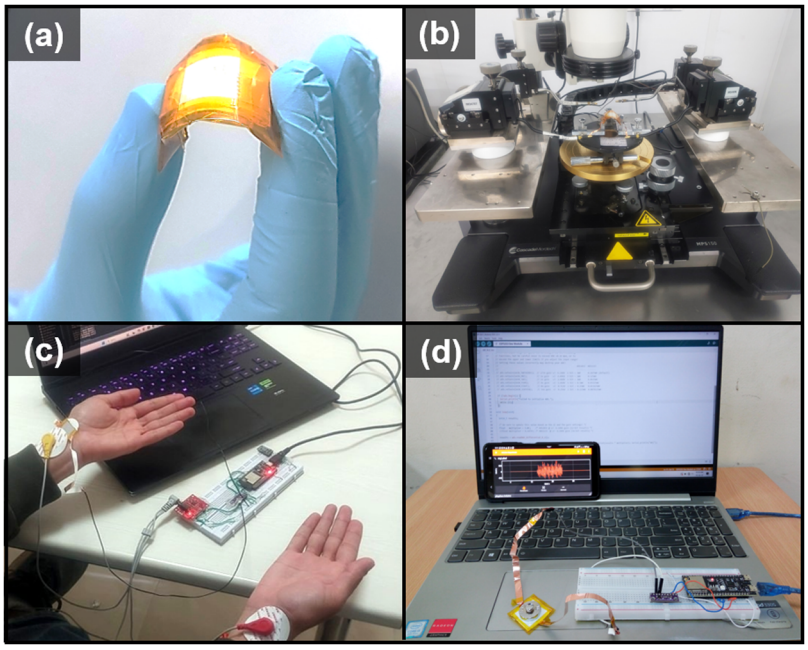

Figure 12. Demonstration of (a) fabricated pressure sensor prototype, (b) pressure sensor prototype measurement employing Keithley 4200A-SCS parameter analyzer, (c) ECG and pulse monitoring configuration, and (d) wireless transmission of pressure sensor data and associated setup.

enhanced electrical conductivity using lithium perchlorate, the developed sensor devices offer a promising solution to the limitations of conventional analogous pressure sensor devices. The pressure sensors fabricated using the P(VDF-TrFE):Li-ClO_4 hybrid nanofibers exhibit superior sensing capability in the low-pressure ranges relative to P(VDF-TrFE) nanofibers while preserving sensing capability in the medium-pressure ranges. Additionally, the prototype devices showed a rapid response and relaxation time (~20−30 ms) and a sensitivity of 6.639 kPa^{-1}. Hybrid nanofibers have shown a substantial ~21% increase in the piezoelectric coefficient (d_{33}) and a notable rise in voltage (~1.4 V) at an optimal $LiClO_4$ concentration of 5 w/v%. The functionality of the developed sensor has been demonstrated by precisely monitoring radial artery pulse pressure and capturing a capacitance versus time waveform that resembles arterial pulse dynamics. Experimental outcomes of this work possess great potential in advancing piezocapacitive nanofibrous devices, which can serve a broad range of applications in energy harvesting, wearable electronics, and real-time health monitoring and pressure sensing technologies.

EXPERIMENTAL SECTION

Materials. P(VDF-TrFE) (Solvene 250/P400, CAS:28960-88-5), lithium perchlorate (CAS:7791-03-9), acetone, and *N*,*N*-dimethylformamide (DMF) were sourced from Sigma-Aldrich (UK). Flexible PET sheets with an ITO coating were purchased from Shilpent. S D Fine-Chem Ltd. supplied the isopropyl alcohol and alkaline liquid soap.

https://doi.org/10.1021/acsaelm.5c00199
ACS Appl. Electron. Mater. XXXX, XXX, XXX−XXX

P(VDF-TrFE) Solution Synthesis. P(VDF-TrFE) polymer in powder form was solubilized in DMF at a weight ratio of 24:56:20 to synthesize the P(VDF-TrFE) solution. After that, the blend was stirred with a magnetic stirrer for at least 7 h at 70 °C on a hot plate. Once the mixture had a uniform viscosity and clear appearance, acetone was added and stirred for a minimum of 4 h without heating. Various weight-by-volume percentages (w/v%) of $LiClO_4$ (1,2, 5, 8 and 10) with respect to P(VDF-TrFE) were then doped into the resulting polymer solution.

Nanofibers Deposition. ITO-coated flexible PET sheets were sonicated for 15 min in each of three different cleaning solutions: soap water, deionized water (DI), and isopropanol. Following cleaning, the sheets were dried by using a nitrogen gun and were subjected to a 20 min UV ozone treatment. The synthesized P(VDF-TrFE):$LiClO_4$ solution was filled into a syringe connected to a syringe pump. Using a Super ES-2 (E-Spin Nanotech) system, the solution was electrospun at a flow rate of 0.7 μL s^{-1}, maintaining a positive 17 kV bias on the needle while the fiber collector remained electrically grounded. Nanofibers were obtained by maintaining the collection roller speed at 800 rpm (rpm) and a distance of 18 cm between the spinneret and the roller. Nanofibers were continually formed on the ITO-coated PET sheets until a consistent layer was obtained.

Piezoresponse Force Microscopy. AFM (Bruker, Dimension ICON PT) was used to analyze both the P(VDF-TrFE) and P(VDF-TrFE):$LiClO_4$ hybrid nanofibers. The PFM measurements were performed by a conducting AFM probe with a diameter of 10 nm, a resonant frequency (f_0) of 75 kHz, and a theoretical spring constant of 3 nm^{-1}. Throughout PFM observations, the mechanical response to an applied electric field was captured by an AFM probe tip, which functioned in contact mode, while an alternating voltage was applied to the tip. The tip recorded the deformation induced by the voltage, and the movements of the cantilever were studied through a lock-in amplifier.

Electrical Characterizations. Electrical characteristics of the P(VDF-TrFE) and P(VDF-TrFE):$LiClO_4$ prototype device structures were measured using a digital storage oscilloscope (DSO1052B, Agilent Technologies) and a Keithley 4200A-SCS parameter analyzer, and the d_{33} coefficient was measured with a YE2730A d_{33} piezometer from APC International Ltd.

Morphological Characterizations. Zeiss Gemini 500 field emission scanning electron microscope was used to capture FESEM images of the nanofibers. For XRD spectra characterization, a SmartLab X-ray diffractometer (Rigaku) was employed. Thermo Scientific (NEXSA Surface Analysis) was used for X-ray photoelectron spectroscopy elemental mapping, and a PerkinElmer FTIR spectrometer was employed for Fourier transform infrared spectroscopy (FTIR).

AUTHOR INFORMATION

Corresponding Author

Satinder K. Sharma − *School of Computing and Electrical Engineering (SCEE), Indian Institute of Technology (IIT)-Mandi, Mandi, Himachal Pradesh 175075, India;* orcid.org/0000-0001-9313-5550; Email: satinder@iitmandi.ac.in

Authors

Pankaj Kumar − *School of Computing and Electrical Engineering (SCEE), Indian Institute of Technology (IIT)-Mandi, Mandi, Himachal Pradesh 175075, India*

Ranbir Singh − *School of Mechanical and Materials Engineering (SMME), Indian Institute of Technology (IIT)-Mandi, Mandi, Himachal Pradesh 175075, India;* orcid.org/0000-0002-5659-478X

Complete contact information is available at: https://pubs.acs.org/10.1021/acsaelm.5c00199

Notes

The authors declare no competing financial interest.

ACKNOWLEDGMENTS

The authors would like to thank the Centre for Design & Fabrication of Electronic Devices (C4DFED) and Advanced Material Research Center (AMRC) at the Indian Institute of Technology Mandi for device fabrication and characterization facilities.

REFERENCES

(1) Lee, J.; Kwon, H.; Seo, J.; Shin, S.; Koo, J. H.; Pang, C.; Son, S.; Kim, J. H.; Jang, Y. H.; Kim, D. E. Conductive fiber-based ultrasensitive textile pressure sensor for wearable electronics. *Adv. Mater.* **2015**, *27* (15), 2433−2439.

(2) Dhakar, L.; Gudla, S.; Shan, X.; Wang, Z.; Tay, F. E. H.; Heng, C.-H.; Lee, C. Large scale triboelectric nanogenerator and self-powered pressure sensor array using low cost roll-to-roll UV embossing. *Sci. Rep.* **2016**, *6* (1), No. 22253.

(3) Lou, Z.; Chen, S.; Wang, L.; Jiang, K.; Shen, G. An ultra-sensitive and rapid response speed graphene pressure sensors for electronic skin and health monitoring. *Nano Energy* **2016**, *23*, 7−14.

(4) Fischer, R.; Müntjes, J. A.; Mokwa, W. *Compensation of the Stress Dependence of Flexible Integrated Capacitive Pressure Sensors for Biomedical Applications*, 2017 IEEE SENSORS, IEEE: 2017; pp 1−3.

(5) Ali, S.; Maddipatla, D.; Narakathu, B. B.; Chlaihawi, A. A.; Emamian, S.; Janabi, F.; Bazuin, B. J.; Atashbar, M. Z. Flexible capacitive pressure sensor based on PDMS substrate and Ga−In liquid metal. *IEEE Sens. J.* **2019**, *19* (1), 97−104.

(6) Maddipatla, D.; Narakathu, B. B.; Ali, M. M.; Chlaihawi, A. A.; Atashbar, M. Z. *Development of a Novel Carbon Nanotube Based Printed and Flexible Pressure Sensor*, IEEE Sensors Applications Symposium (SAS), IEEE: 2017; pp 1−4.

(7) Kumar, M.; Choudhary, S.; Sharma, S. K.; Randhawa, J. K. Piezoelectric nanogenerators with hybrid nanofibers: a dual approach for energy generation and wastewater treatment. *Environ. Sci.:Nano* **2025**, *12*, 1431−1445, DOI: 10.1039/D4EN00568F.

(8) Chen, L.; Liu, J.; Wang, X.; Ji, B.; Chen, X.; Yang, B. Flexible capacitive hydrogel tactile sensor with adjustable measurement range using liquid crystal and carbon nanotubes composites. *IEEE Trans. Electron Devices* **2017**, *64* (5), 1968−1972.

(9) Sharafkhani, S.; Kokabi, M. Enhanced sensing performance of polyvinylidene fluoride nanofibers containing preferred oriented carbon nanotubes. *Adv. Compos. Hybrid Mater.* **2022**, *5* (4), 3081−3093.

(10) Wang, B.; Wang, J.; Lou, Y.; Ding, S.; Jin, X.; Liu, F.; Xu, Z.; Ma, J.; Sun, Z.; Li, X. Halloysite nanotubes strengthened electrospinning composite nanofiber membrane for on-skin flexible pressure sensor with high sensitivity, good breathability, and round-the-clock antibacterial activity. *Appl. Clay Sci.* **2022**, *228*, No. 106650.

(11) Atalay, O.; Atalay, A.; Gafford, J.; Walsh, C. A highly sensitive capacitive-based soft pressure sensor based on a conductive fabric and a microporous dielectric layer. *Adv. Mater. Technol.* **2018**, *3* (1), No. 1700237.

(12) Zou, Y.; Chen, Z.; Guo, X.; Peng, Z.; Yu, C.; Zhong, W. Mechanically robust and elastic graphene/aramid nanofiber/polyaniline nanotube aerogels for pressure sensors. *ACS Appl. Mater. Interfaces* **2022**, *14* (15), 17858−17868.

(13) Abolhasani, M. M.; Azimi, S.; Mousavi, M.; Anwar, S.; Hassanpour Amiri, M.; Shirvanimoghaddam, K.; Naebe, M.; Michels, J.; Asadi, K. Porous graphene/poly (vinylidene fluoride) nanofibers for pressure sensing. *J. Appl. Polym. Sci.* **2022**, *139* (14), No. 51907.

(14) Javidi, R.; Moghimi Zand, M.; Alizadeh Majd, S. Designing wearable capacitive pressure sensors with arrangement of porous pyramidal microstructures. *Micro Nano Syst. Lett.* **2023**, *11* (1), No. 13.

(15) Liu, S.-Y.; Lu, J.-G.; Shieh, H.-P. D. Influence of permittivity on the sensitivity of porous elastomer-based capacitive pressure sensors. *IEEE Sens. J.* **2018**, *18* (5), 1870−1876.
(16) Wang, D.; Wang, L.; Shen, G. Nanofiber/nanowires-based flexible and stretchable sensors. *J. Semicond.* **2020**, *41* (4), No. 041605.
(17) Zhong, W.; Liu, C.; Liu, Q.; Piao, L.; Jiang, H.; Wang, W.; Liu, K.; Li, M.; Sun, G.; Wang, D. Ultrasensitive wearable pressure sensors assembled by surface-patterned polyolefin elastomer nanofiber membrane interpenetrated with silver nanowires. *ACS Appl. Mater. Interfaces* **2018**, *10* (49), 42706−42714.
(18) Cheng, W.; Wang, J.; Ma, Z.; Yan, K.; Wang, Y.; Wang, H.; Li, S.; Li, Y.; Pan, L.; Shi, Y. Flexible pressure sensor with high sensitivity and low hysteresis based on a hierarchically microstructured electrode. *IEEE Electron Device Lett.* **2018**, *39* (2), 288−291.
(19) Hu, X.; Jiang, Y.; Ma, Z.; He, Q.; He, Y.; Zhou, T.; Zhang, D. Highly sensitive P (VDF-TrFE)/BTO nanofiber-based pressure sensor with dense stress concentration microstructures. *ACS Appl. Polym. Mater.* **2020**, *2* (11), 4399−4404.
(20) Thouti, E.; Nagaraju, A.; Chandran, A.; Prakash, P.; Shivanarayanamurthy, P.; Lal, B.; Kumar, P.; Kothari, P.; Panwar, D. Tunable flexible capacitive pressure sensors using arrangement of polydimethylsiloxane micro-pyramids for bio-signal monitoring. *Sens. Actuators, A* **2020**, *314*, No. 112251.
(21) Mannsfeld, S. C.; Tee, B. C.; Stoltenberg, R. M.; Chen, C. V. H.; Barman, S.; Muir, B. V.; Sokolov, A. N.; Reese, C.; Bao, Z. Highly sensitive flexible pressure sensors with microstructured rubber dielectric layers. *Nat. Mater.* **2010**, *9* (10), 859−864.
(22) Tang, R.; Lu, F.; Liu, L.; Yan, Y.; Du, Q.; Zhang, B.; Zhou, T.; Fu, H. Flexible pressure sensors with microstructures. *Nano Sel.* **2021**, *2* (10), 1874−1901.
(23) Park, J.; Kim, J.; Hong, J.; Lee, H.; Lee, Y.; Cho, S.; Kim, S.-W.; Kim, J. J.; Kim, S. Y.; Ko, H. Tailoring force sensitivity and selectivity by microstructure engineering of multidirectional electronic skins. *NPG Asia Mater.* **2018**, *10* (4), 163−176.
(24) Wen, Z.; Yang, J.; Ding, H.; Zhang, W.; Wu, D.; Xu, J.; Shi, Z.; Xu, T.; Tian, Y.; Li, X. Ultra-highly sensitive, low hysteretic and flexible pressure sensor based on porous MWCNTs/Ecoflex elastomer composites. *J. Mater. Sci.:Mater. Electron.* **2018**, *29*, 20978−20983.
(25) Lee, B.-Y.; Kim, J.; Kim, H.; Kim, C.; Lee, S.-D. Low-cost flexible pressure sensor based on dielectric elastomer film with micro-pores. *Sens. Actuators, A* **2016**, *240*, 103−109.
(26) Yang, X.; Wang, Y.; Qing, X. A flexible capacitive sensor based on the electrospun PVDF nanofiber membrane with carbon nanotubes. *Sens. Actuators, A* **2019**, *299*, No. 111579.
(27) Tang, Y.; Zhang, T.; Ren, H.; Zhang, W.; Li, G.; Guo, D.; Yang, L.; Tan, R.; Shen, Y. Highly sensitive spherical cap structure-based iontronic pressure sensors by a mold-free fabrication approach. *Smart Mater. Struct.* **2022**, *31* (9), No. 095030.
(28) Bano, S.; Gupta, B.; Sharma, S. K.; Singh, R. Coupling of triboelectric and piezoelectric effects in nafion-containing polyvinylidene fluoride: lead zirconium titanate nanofiber-based nanogenerators for self-powered systems. *ACS Appl. Nano Mater.* **2024**, *7* (13), 15425−15437.
(29) Sharma, S.; Das, S.; Khosla, R.; Shrimali, H.; Sharma, S. K. Highly UV sensitive Sn nanoparticles blended with polyaniline onto micro-interdigitated electrode array for UV-C detection applications. *J. Mater. Sci.:Mater. Electron.* **2019**, *30*, 7534−7542.
(30) Veved, A.; Ejuh, G. W.; Djongyang, N. Review of emerging materials for PVDF-based energy harvesting. *Energy Rep.* **2022**, *8*, 12853−12870.
(31) Gao, X.; Zhou, F.; Li, M.; Wang, X.; Chen, S.; Yu, J. Flexible stannum-doped SrTiO3 nanofiber membranes for highly sensitive and reliable piezoresistive pressure sensors. *ACS Appl. Mater. Interfaces* **2021**, *13* (44), 52811−52821.
(32) Cao, H.; Chai, S.; Tan, Z.; Wu, H.; Mao, X.; Wei, L.; Zhou, F.; Sun, R.; Liu, C. Recent advances in physical sensors based on electrospinning technology. *ACS Mater. Lett.* **2023**, *5* (6), 1627−1648.
(33) Ghosh, R.; Pin, K. Y.; Reddy, V. S.; Jayathilaka, W.; Ji, D.; Serrano-García, W.; Bhargava, S. K.; Ramakrishna, S.; Chinnappan, A. Micro/nanofiber-based noninvasive devices for health monitoring diagnosis and rehabilitation. *Appl. Phys. Rev.* **2020**, *7* (4), No. 041309, DOI: 10.1063/5.0010766.
(34) Kumar, P.; Choudhary, S.; Sharma, K. P.; Sharma, S. K.; Singh, R. Light-Sensitive PVDF-TrFE: PDI Hybrid Nanofibers-Based Flexible Bimodal Piezoelectric Nanogenerator. *IEEE J. Flexible Electron.* **2022**, *1* (3), 194−202.
(35) Sudiarti, T.; Wahyuningrum, D.; Bundjali, B.; Arcana, I. M. *Mechanical Strength and Ionic Conductivity of Polymer Electrolyte Membranes Prepared from Cellulose Acetate-lithium Perchlorate*, IOP Conference Series: Materials Science and Engineering, IOP Publishing: 2017; p 012052.
(36) Das, S.; Prathapa, S. J.; Menezes, P. V.; Row, T. N. G.; Bhattacharyya, A. J. Study of ion transport in lithium perchlorate-succinonitrile plastic crystalline electrolyte via ionic conductivity and in situ cryo-crystallography. *J. Phys. Chem. B* **2009**, *113* (15), 5025−5031.
(37) Baniasadi, M.; Xu, Z.; Hong, S.; Naraghi, M.; Minary-Jolandan, M. Thermo-electromechanical behavior of piezoelectric nanofibers. *ACS Appl. Mater. Interfaces* **2016**, *8* (4), 2540−2551.
(38) Wu, L.; Jin, Z.; Liu, Y.; Ning, H.; Liu, X.; Alamusi; Hu, N. Recent advances in the preparation of PVDF-based piezoelectric materials. *Nanotechnol. Rev.* **2022**, *11* (1), 1386−1407.
(39) Ansari, M. Z.; Banitaba, S. N.; Khademolqorani, S.; Kamika, I.; Jadhav, V. V. Overlooked promising green features of electrospun cellulose-based fibers in lithium-ion batteries. *ACS Omega* **2023**, *8* (46), 43388−43407.
(40) Reddy, V. S.; Tian, Y.; Zhang, C.; Ye, Z.; Roy, K.; Chinnappan, A.; Ramakrishna, S.; Liu, W.; Ghosh, R. A review on electrospun nanofibers based advanced applications: From health care to energy devices. *Polymers* **2021**, *13* (21), No. 3746.
(41) Li, X.; Wang, Y.; He, T.; Hu, Q.; Yang, Y. Preparation of PVDF flexible piezoelectric film with high β-phase content by matching solvent dipole moment and crystallization temperature. *J. Mater. Sci.:Mater. Electron.* **2019**, *30*, 20174−20180.
(42) Darestani, M. T.; Coster, H.; Chilcott, T. C.; Fleming, S.; Nagarajan, V.; An, H. Piezoelectric membranes for separation processes: Fabrication and piezoelectric properties. *J. Membr. Sci.* **2013**, *434*, 184−192.
(43) Liu, X.; Xu, S.; Kuang, X.; Tan, D.; Wang, X. Nanoscale investigations on β-phase orientation, piezoelectric response, and polarization direction of electrospun PVDF nanofibers. *RSC Adv.* **2016**, *6* (110), 109061−109066.
(44) Zeng, Y.; Qin, Y.; Yang, Y.; Lu, X. A low-cost flexible capacitive pressure sensor for health detection. *IEEE Sens. J.* **2022**, *22* (8), 7665−7673.
(45) Ma, L.; Shuai, X.; Hu, Y.; Liang, X.; Zhu, P.; Sun, R.; Wong, C.-p. A highly sensitive and flexible capacitive pressure sensor based on a micro-arrayed polydimethylsiloxane dielectric layer. *J. Mater. Chem. C* **2018**, *6* (48), 13232−13240.
(46) Lv, C.; Tian, C.; Jiang, J.; Dang, Y.; Liu, Y.; Duan, X.; Li, Q.; Chen, X.; Xie, M. Ultrasensitive linear capacitive pressure sensor with wrinkled microstructures for tactile perception. *Adv. Sci.* **2023**, *10* (14), No. 2206807.
(47) Xu, J.; Li, H.; Yin, Y.; Li, X.; Cao, J.; Feng, H.; Bao, W.; Tan, H.; Xiao, F.; Zhu, G. High sensitivity and broad linearity range pressure sensor based on hierarchical in-situ filling porous structure. *npj Flexible Electron.* **2022**, *6* (1), No. 62.
(48) Zhao, T.; Li, T.; Chen, L.; Yuan, L.; Li, X.; Zhang, J. Highly sensitive flexible piezoresistive pressure sensor developed using biomimetically textured porous materials. *ACS Appl. Mater. Interfaces* **2019**, *11* (32), 29466−29473.
(49) Huang, W.; Dai, K.; Zhai, Y.; Liu, H.; Zhan, P.; Gao, J.; Zheng, G.; Liu, C.; Shen, C. Flexible and lightweight pressure sensor based on carbon nanotube/thermoplastic polyurethane-aligned conductive

foam with superior compressibility and stability. *ACS Appl. Mater. Interfaces* **2017**, *9* (48), 42266−42277.

https://doi.org/10.1021/acsaelm.5c00199
ACS Appl. Electron. Mater. XXXX, XXX, XXX−XXX